



Nitrogen-doped carbon catalysts derived from ionic liquids in the presence of transition metals for the oxygen reduction reaction



Katie H. Lim, Hansung Kim*

Dept. of Chemical and Biomolecular Engineering, Yonsei University 50 Yonsei-ro Seodaemun-gu, 120-749 Seoul, Republic of Korea

ARTICLE INFO

Article history:

Received 19 January 2014

Received in revised form 10 April 2014

Accepted 23 April 2014

Available online 2 May 2014

Keywords:

Non-precious catalyst

Nitrogen doped carbon

Ionic liquid

Oxygen reduction reaction

sp² Carbon network

ABSTRACT

Nitrogen-doped carbon catalysts for the oxygen reduction reaction (ORR) were synthesized by the pyrolysis of ionic liquids (IL), which are precursors of both nitrogen and carbon, using a silica hard template in the presence of a transition metal. From the linear sweep voltammogram recorded in an acidic solution, the ORR activity of the nitrogen-doped carbon catalysts increased significantly after the addition of the transition metal during the pyrolysis of the IL. From XPS-N 1s analysis, the introduction of the transition metal positively contributes to the formation of graphitic-N, which is known to be an active site for the ORR. The results of XPS-C 1s suggest a strong correlation between the sp²-carbon network and the ORR activity. Co is a more effective metal compared to Ni due to the creation of a higher degree of sp²-carbon networks for fast electron transfer during the ORR. Based on the quantitative analysis of the experimental results, the IL is a promising precursor for nitrogen-doped carbon catalysts, and the addition of a transition metal is essential for improved activity of the ORR.

© 2014 Elsevier B.V. All rights reserved.

1. Introduction

Polymer electrolyte membrane fuel cells (PEMFCs) have been recognized as potential electricity generating devices with a low environmental impact and high efficiency especially for application as automotive and stationary power sources [1–3]. Because PEMFCs are a type of electrochemical device, electrocatalysts play important roles in determining the performances of PEMFCs. Conventionally, Pt-based catalysts are commonly used as catalysts on both the cathode and the anode. Because the rate of the oxygen reduction reaction (ORR) occurring at the cathode is much slower than the rate of the hydrogen oxidation reaction at anode, the cathode requires much larger quantities of precious catalysts [4]. Therefore, a high cost and a limited supply of Pt have prevented the successful commercialization of PEMFCs.

Among the various alternatives for Pt-based catalysts [5–10], carbon-based materials, especially nitrogen-doped carbon, are of great interest as non-precious metal catalysts for the ORR due to their relatively high activity and superior stability [11–16]. Li et al. demonstrated that the presence of nitrogen on the carbon nanotube (CNT) induces a high ORR activity that is comparable to Pt based

catalysts in an alkaline medium [17]. The multi-walled N-doped CNT containing 8.4 at.% nitrogen exhibited a high ORR catalytic activity as well as an improved stability due to the durable physical characteristics of the CNTs. In an effort to enhance the catalytic activity of nitrogen-doped carbon, transition metals were introduced to nitrogen containing complexes [18–21]. The transition metal itself does not participate in the ORR but serves to catalyze the formation of nitrogen-doping structures in the carbon framework that are active toward the ORR [13,22,23]. Therefore, the nitrogen content and doping structure in the carbon materials are expected to be a governing factor for the ORR activity.

In this regard, several attempts have been made to increase the nitrogen content in carbon based materials by employing precursors with a high nitrogen content, such as ionic liquids (ILs) [24–27]. A variety of ionic liquids were investigated as precursors for the preparation of nitrogen-doped carbon [28], and additives were incorporated as a nitrogen donor to increase the nitrogen content of the material [29]. However, relatively little work has been dedicated to investigating the effect of transition metals on the formation of nitrogen functional groups when IL are used as precursors and the activity of these catalysts for the ORR, especially in acidic media.

Therefore, we experimentally examined the ORR activity of nitrogen-doped carbon materials prepared by pyrolysis of ionic liquids (i.e., 1-ethyl-3-methylimidazolium dicyanamide (C₈H₁₁N₅,

* Corresponding author. Tel.: +82 2 2123 5753; fax: +82 2 312 6401.
E-mail address: elchem@yonsei.ac.kr (H. Kim).

Emim-dca) as a nitrogen and carbon precursor) in the presence of various transition metals. Based on the results, the effect of the transition metal on the activity of the ORR was investigated, and the enhanced ORR activity was correlated with the nitrogen-doped structure and sp^2 degree of carbon network in the nitrogen-doped carbon catalysts.

2. Experimental

2.1. Catalyst synthesis

The nitrogen-doped carbon-based catalysts investigated in this paper were synthesized by the pyrolysis of a mixture consisting of an ionic liquid, silica suspension, and transition metal salts. In detail, an ionic liquid (i.e., 1-ethyl-3-methylimidazolium dicyanamide ($C_8H_{11}N_5$, Emim-dca)), which is composed of only C, H, and N, acts as a nitrogen and carbon precursor, and silica suspension and transition metal salts are employed as hard template and nitrogen-doping aide, respectively. Initially, different amounts of a cobalt salt ($Co(NO_3)_2 \cdot 6H_2O$) were dissolved in de-ionized water to prepare catalysts containing different Co loadings (i.e., 5, 10, 15 wt.%). This ratio indicates the proportion of cobalt to the carbon carbonized from the ionic liquid. Next, Emim-dca (1 g, from BASF) and a silica suspension (2.5 g, LUDOX HS40) were added to the dissolved Co solution followed by ultra-sonication to uniformly disperse the silica template in the solution. The resulting homogeneous mixture was pyrolyzed under argon in two steps. First, the mixture was pyrolyzed for 1 h at $300^\circ C$ to completely remove the water, and then, the mixture was pyrolyzed for an additional 1 h at $800^\circ C$ to carbonize the sample. After the pyrolysis, the black powder was treated with a HF solution for 3 h to leach out the excess metal elements and etch the silica templates, which was thoroughly washing several times with de-ionized water. The catalyst was dried in a vacuum oven at $80^\circ C$ overnight, and each resulting catalyst was denoted IL + Si + CoM, where M indicates the metal content (wt.%) of the sample. For comparison, IL, IL + Co10 and IL + Si were also synthesized by the procedure mentioned above except that the silica suspension and cobalt nitrate, respectively. Nickel nitrate ($Ni(NO_3)_2 \cdot 6H_2O$) was also applied as a transition metal salt instead of cobalt nitrate to determine the effect of different transition metal. The sample with different transition metal, Ni, was synthesized with 10 wt.% of transition metal and denoted as IL + Si + Ni10.

2.2. Electrochemical characterization

The electrochemical properties of the prepared nitrogen-doped carbon-based catalysts were analyzed using a rotating ring-disk electrode (RRDE, Pine Research Instruments). The experiments were conducted using a conventional three-electrode system equipped with a platinum wire counter electrode and a Hg/Hg_2SO_4 reference electrode in a 0.5 M H_2SO_4 electrolyte. For the working electrode, the prepared catalyst was coated onto a glassy carbon electrode as a thin film. The catalyst ink was prepared by the method described in our previous study on N-doped carbon [30]. 8 mg of the catalyst powder was ultrasonically dispersed in a solution containing 0.5 mL of isopropyl alcohol (IPA), 1.5 mL of de-ionized water and 50 μL of 5 wt.% Nafion solution. Then, the catalyst ink (15 μL) was dropped onto the glassy carbon disk of the RRDE, which was followed by drying in a nitrogen atmosphere at room temperature. Linear-sweep voltammograms were recorded in the potential range between 1.0 and 0.0 V_{SHE} at a scan rate of $5 mV s^{-1}$ and a rotating speed of 1200 rpm.

Table 1

BET and ICP analysis of the prepared catalysts. ICP was obtained before and after acidic leaching in a HF solution for 3 h.

| | Specific surface area ($m^2 g^{-1}$) | Co content (wt.%) | |
|----------------|--|-------------------|----------------|
| | | Before leaching | After leaching |
| IL | 3.41 | – | – |
| IL + Si | 1309 | – | – |
| IL + Si + Co5 | 975 | 4.2 | 3.2 |
| IL + Si + Co10 | 824 | 8.3 | 2.6 |
| IL + Si + Co15 | 645 | 13.2 | 2.2 |

2.3. Physical characterization

High-resolution transmission electron microscopy (HR-TEM, JEM-30100 model) was performed to observe the morphology of the carbon structure. Photoelectron spectroscopy (XPS, K-alpha, Thermo, UK) was performed to analyze the surface composition of the catalysts. The nitrogen content in the bulk samples was measured using an elemental analyzer (EA, 2400 Series II CHNS/O Analyzer, PerkinElmer Co., USA). The transition metal loading that remained in each catalyst was estimated using an inductively coupled plasma-atomic emission spectroscopy (ICP-AES) analysis. Brunauer–Emmett–Teller (BET) nitrogen adsorption isotherms were recorded using on a Micromeritics TriStar analyzer at 77 K.

3. Results and discussion

HR-TEM analysis was performed to characterize the morphologies of the nitrogen-doped carbons prepared by the pyrolysis of the IL using the silica template (IL + Si) and the addition of a transition metal (IL + Si + Co10). As shown in Fig. 1a, the nitrogen-doped carbon synthesized by pyrolysis of the IL without any additives resulted in a thin carbon sheet without pores. However, the morphology of the catalyst changed after the introduction of 12 nm silica nanoparticles (LUDOX-HS40), which were used as a hard template, as shown in Fig. 1b. It can be clearly observed that the removal of silica particles using the acidic etching process creates a highly porous structure in the nitrogen-doped carbon. The specific surface area determined by BET analysis significantly increases from $3.41 m^2 g^{-1}$ to $1309 m^2 g^{-1}$ after application of the silica template. Because the HR-TEM images of Fig. 1b and c are quite similar, the addition of Co to the IL + Si catalyst does not drastically change the porous structure. However, the specific surface area decreases linearly to $645 m^2 g^{-1}$ as the amount of added cobalt increases from 0 wt.% to 15 wt.%. According to the ICP measurement used to quantify the Co content before and after the chemical leaching process, the initial Co content was close to the nominal target, as shown in Table 1. In contrast, after chemical leaching, the residual Co content appears to be nearly same between 2.2 and 3.2 wt.% regardless of the initial Co content. The metallic Co that survived the severe chemical leaching process is primarily due to the formation of a barrier, such as encapsulation of the carbon layers during the pyrolysis process [22,31]. Therefore, the reduced specific surface area upon addition of Co is not associated with the residual Co content.

The ORR catalytic activities for the nitrogen-doped carbon catalysts synthesized from IL were evaluated by linear sweep voltammetry using a rotating ring disk electrode system in a 0.5 M O_2 -saturated H_2SO_4 solution. As shown in Fig. 2, the lowest ORR activity was observed for the catalyst prepared by the pyrolysis of the IL only. After application of the silica nanoparticles as a hard template, the ORR catalytic activity improved due to the increased surface area, which was determined from the BET results. It is important to note that a dramatic improvement in the activity was observed with the simultaneous addition of the silica template and Co. The ORR activity increases with addition of Co up to 10 wt.%

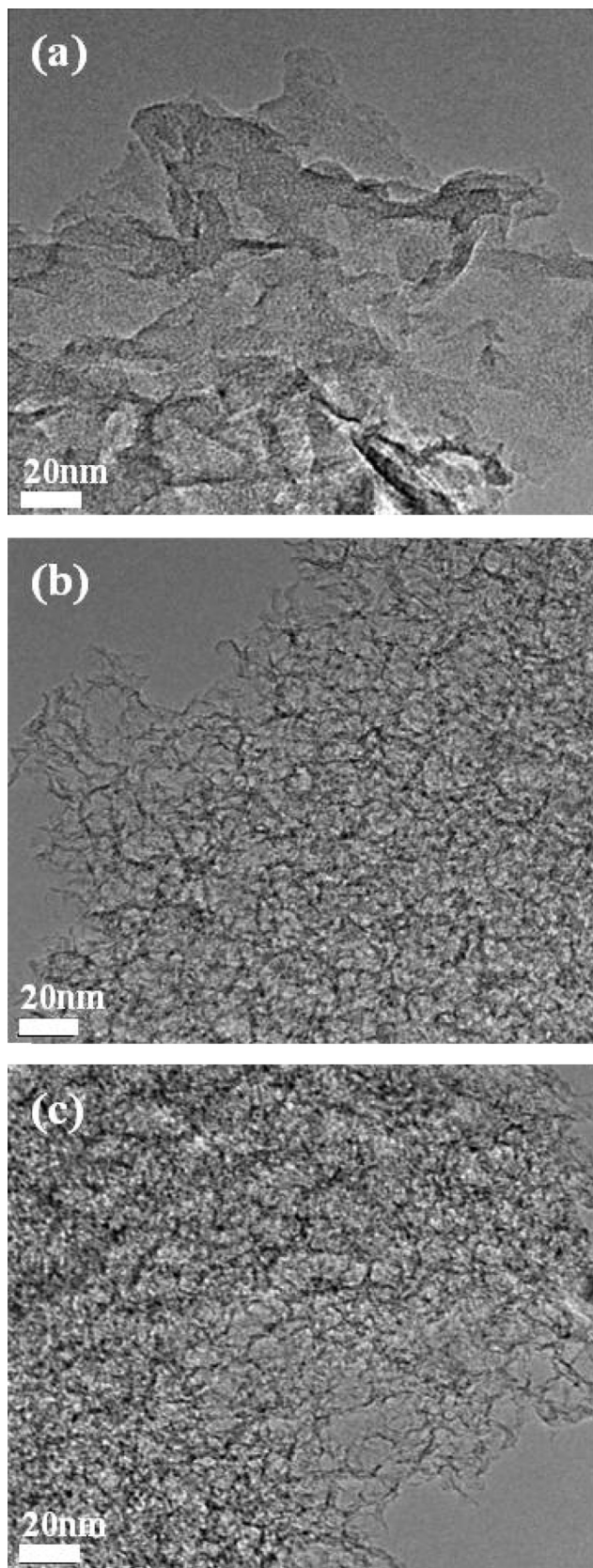


Fig. 1. HR-TEM images of the prepared catalysts for (a) IL, (b) IL+Si and (c) IL+Si+Co10.

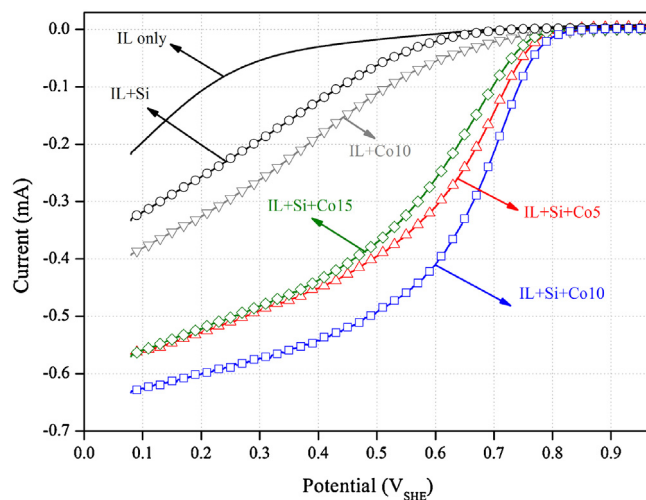


Fig. 2. Polarization curves for oxygen reduction on the nitrogen-doped carbon catalysts with different Co contents. For comparison, IL, IL+Si and IL+Co10 are also shown. The measurements were performed in an O_2 -saturated 0.5 M H_2SO_4 solution using a potential scan rate of 5 mV s^{-1} and a rotation speed of 1200 rpm.

and then decreases with a further increase in the Co content (i.e., 15 wt.%). By comparing the IL+Si and IL+Si+Co10 catalysts, the onset potential shifted in a positive direction by 0.15 V, and the ORR current increased from 0.011 mA to 0.349 mA at 0.6 V_{SHE} . For comparison, the IL+Co10 without application of silica nanoparticles was prepared to examine the effect of surface area on the catalytic activity. The BET of IL+Co10 was measured to be $172 \text{ m}^2 \text{ g}^{-1}$ which is much lower than that of IL+Si+Co10. As a result, the ORR catalytic activity of IL+Co10 was poor compared to IL+Si+Co10 indicating that the active surface area is important to enhance the catalytic activity.

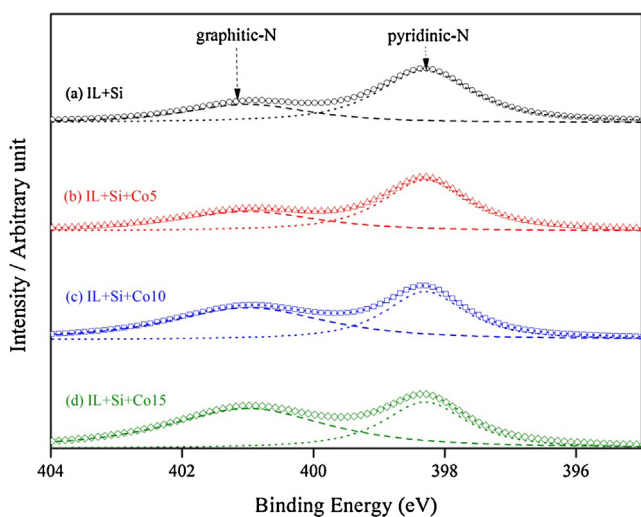
To understand the role of Co in more detail, the total nitrogen content of each catalyst was measured by an elemental analyzer (EA). According to the EA data listed in Table 2, high nitrogen content (9.05–21.04 wt.% of N) was achieved by using the IL as a nitrogen precursor. The IL provide much higher nitrogen content compared to the other reported nitrogen-doped carbon materials, which are typically less than 5 wt.% [12,22,32]. Therefore, it is apparent that the use of IL as a nitrogen precursor is an efficient method for preparing nitrogen rich carbon catalysts. By comparing the nitrogen content listed in Table 2, the IL+Si catalyst, which as the lowest ORR activity, has the highest nitrogen content indicating that the total amount of nitrogen is not the only factor determining the high ORR activity. Therefore, it is necessary to analyze the nitrogen-doping structures in the nitrogen-doped carbon catalysts using XPS.

Fig. 3 shows the result from the N 1s spectra of the catalysts that are decomposed into two dominant peaks corresponding to pyridinic-N and graphitic-N [33,34]. The nitrogen content and relative composition ratio of the two different nitrogen-doped structures are also summarized in Table 2. Nitrogen doping in the carbon structures occurs at various sites during pyrolysis leading to distinct binding energies. When the nitrogen atoms replace carbon atoms at the edges of the graphitic carbon layers, it is referred to as a pyridinic-N bond to two carbon atoms with a binding energy of $398.6 \pm 0.3 \text{ eV}$ [35]. The graphitic-N type is a nitrogen with three carbon neighbors that is doped inside the graphitic carbon layer with a relatively higher binding energy of $401.3 \pm 0.3 \text{ eV}$ [36]. As shown in Table 2, the total content of nitrogen measured from XPS is quite similar to the EA results, which indicates that there is no visible difference in the composition of the surface and bulk phase of the catalyst. In addition, as the cobalt content increases

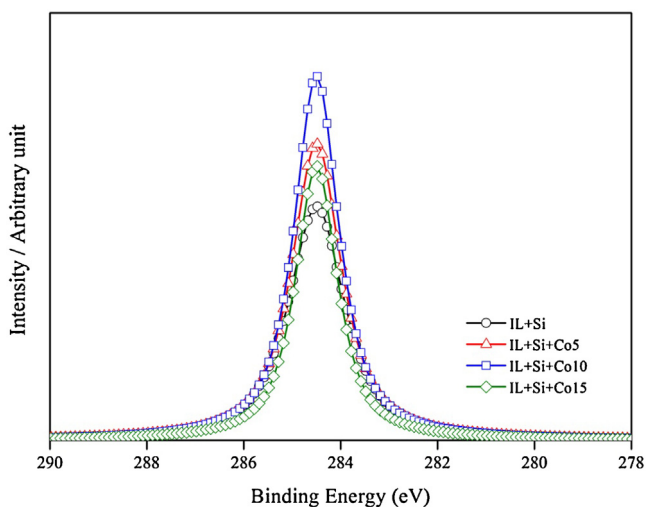
Table 2

Bulk composition and relative composition of nitrogen functional groups obtained from EA and XPS analysis.

| | EA Total N (wt.%) | XPS Total N (wt.%) | Pyridinic-N (%) | Graphitic-N (%) |
|----------------|----------------------|-----------------------|-----------------|-----------------|
| IL + Si | 21.04 | 19.43 | 68.5 | 31.5 |
| IL + Si + Co5 | 17.93 | 19.72 | 61.7 | 38.3 |
| IL + Si + Co10 | 11.75 | 11.24 | 44.6 | 55.4 |
| IL + Si + Co15 | 9.05 | 11.56 | 38.8 | 61.2 |

**Fig. 3.** Deconvoluted XPS spectra of the N 1s region for (a) IL + Si, (b) IL + Si + Co5, (c) IL + Si + Co10 and (d) IL + Si + Co15.

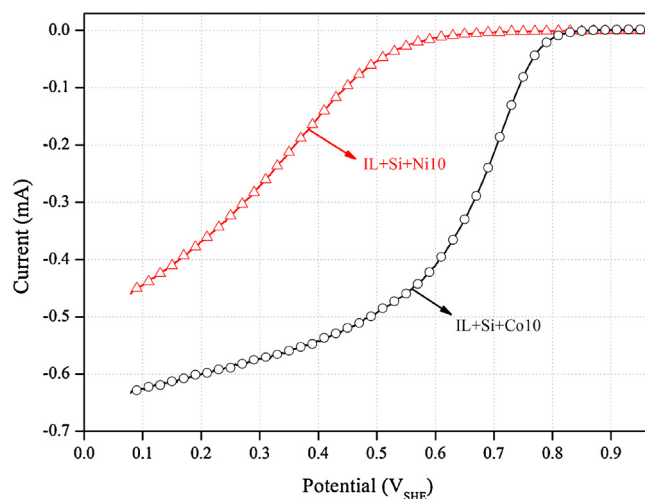
during pyrolysis of the IL, the amount of pyridinic-N decreases from 68.5% to 38.8%, and the amount of graphitic-N increase from 31.5% to 61.2%. It has been reported that a carbon atom next to a graphitic-N especially at the zig-zag edge facilitates adsorption of oxygen molecules and contributes to enhanced ORR catalytic activity [36,37]. Therefore, in the presence of Co, nitrogen atoms are more likely to replace carbon atoms located in the interior rather than at the edge of the graphene layer during pyrolysis of the IL resulting in a higher ORR catalytic activity. However, this argument does not explain the lower ORR activity when the content of Co is increased to 15 wt.%. To explain this result, C 1s spectra of the catalysts were obtained, as shown in Fig. 4. All of the catalysts exhibited a peak at approximately 284.5 eV, which indicates that

**Fig. 4.** XPS-C 1s data of the prepared catalyst as a function of Co content.

primarily C–C bonding in a typical sp^2 carbon network is present. According to the XPS-C 1s results, the ORR activity appears to be closely correlated with the degree of sp^2 -bonding in the structure because the intensities corresponding to sp^2 -bonding agrees well with the order of ORR activity of the catalysts. The intensity of the C 1s peak for IL+Si+Co15 is lower than that of IL+Si+Co5 and IL+Si+Co10, which implies a decrease in the sp^2 -carbon structure. It is well known that the formation of a sufficient sp^2 -carbon network is necessary to provide an effective electron path during ORR [14,18,36]. Therefore, a lower degree of sp^2 hybridization in the IL + Si + Co15 catalyst is responsible for the decreased ORR catalytic activity. Therefore, it can be concluded that the addition of a transition metal to the IL during pyrolysis contributes to the improvement of ORR activity by increasing graphitic-N and the degree of sp^2 -bonding in the carbon structure.

To investigate the effect of a different transition metal, nitrogen-doped carbon was synthesized using the same process in the presence of Ni. The content of the introduced transition metal was fixed at 10 wt.%. The ORR activity of the prepared catalyst was measured by linear sweep voltammetry using a rotating ring disk electrode system. As shown in Fig. 5, the Co containing catalyst exhibits a more positive onset potential and higher catalytic activity toward ORR compared to the catalyst prepared with Ni. Based on this observation, Co is a more favorable transition metal for the fabrication of nitrogen-doped carbon catalyst from the pyrolysis of IL.

To illustrate the enhanced ORR activity of the Co containing catalyst, an XPS-N 1s analysis was performed, and the results are shown in Fig. 6. Interestingly, similar XPS spectra were obtained for all of the catalysts. As shown in Table 3, the ratio of nitrogen doping types is not significantly affected by the type of transition metal indicating that the nitrogen doping type is not the only factor affecting the difference in the ORR activity. From the XPS-C 1s data in Fig. 7,

**Fig. 5.** Polarization curves for oxygen reduction on the nitrogen-doped carbon catalysts with different transition metals. The measurements were performed in an O_2 -saturated 0.5 M H_2SO_4 solution using a potential scan rate of 5 mV s^{-1} and a rotation speed of 1200 rpm.

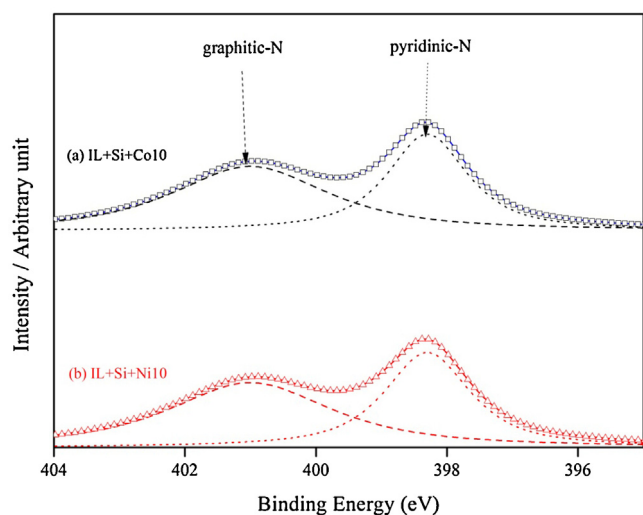


Fig. 6. Deconvoluted XPS spectra of the N 1s region for (a) IL+Si+Co10 and (b) IL+Si+Ni10.

Table 3

Relative composition of nitrogen functional groups obtained from XPS analysis with different transition metals.

| | XPS | |
|------------|-----------------|-----------------|
| | Pyridinic-N (%) | Graphitic-N (%) |
| IL+Si+Co10 | 44.6 | 55.4 |
| IL+Si+Ni10 | 44.5 | 55.5 |

the C–C bonding peak intensity for IL+Si+Co10 is higher than that for IL+Si+Ni10, which indicates a greater sp^2 carbon network is formed in the Co derived nitrogen-doped carbon catalyst compared to the other catalyst. The order of C–C bonding peak is consistent with the ORR catalytic activity shown in Fig. 5, implying the importance of the carbon structures. Therefore, when nitrogen-doped carbon catalysts for ORR are prepared by pyrolysis of high nitrogen containing precursor (i.e., IL), sufficient sp^2 -bonding formation in the carbon structure is critical for fast electron transfer during ORR, and it is strongly affected by the type of transition metal that is added during the pyrolysis process.

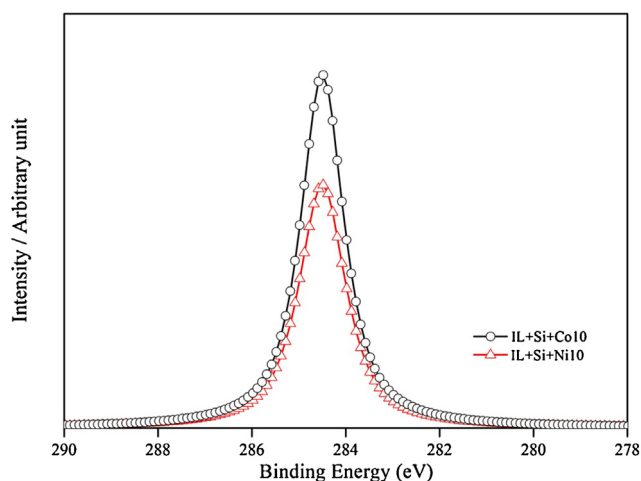


Fig. 7. XPS-C 1s data of the prepared catalyst with different transition metal.

4. Conclusions

Nitrogen-doped carbon catalysts were synthesized by pyrolyzing an ionic liquid (IL) with a silica hard template and transition metal. The effect of the transition metal content and type on the ORR activity of nitrogen-doped carbon catalysts was explored by electrochemical measurement and XPS analysis. The introduction of an optimum amount of Co during the pyrolysis of the IL creates a large amount of graphitic-N and high degree of sp^2 -carbon network, which is favorable for improving the ORR catalytic activity by providing active sites for the ORR and an effective electron path during the ORR. In comparison to Ni, Co derived nitrogen-doped carbon catalysts exhibited a much higher ORR activity, which was primarily due to the formation of a higher degree of sp^2 -carbon network. Therefore, the IL is a promising source of both nitrogen and carbon in the preparation of nitrogen-doped carbon catalysts for the ORR, and the use of a transition metal is essential for preparing highly active catalysts by increasing the concentration of graphitic-N in the sp^2 -carbon network.

Acknowledgements

This work was supported by the Priority Research Centers Program through the National Research Foundation of Korea (2009-0093823) and (NRF-2009-C1AAA001-0092926) funded by the Ministry of Education, Science and Technology.

References

- [1] H.A. Gasteiger, S.S. Kocha, B. Sompalli, F.T. Wagner, *Appl. Catal., B: Environ.* 56 (2005) 9–35.
- [2] T.A. Semelsberger, R.L. Borup, *Int. J. Hydrogen Energy* 30 (2005) 425–435.
- [3] A. Bauen, D. Hart, *J. Power Sources* 86 (2000) 482–494.
- [4] X. Yu, S. Ye, *J. Power Sources* 172 (2007) 133–144.
- [5] J.L. Fernández, V. Raghuveer, A. Manthiram, A.J. Bard, *J. Am. Chem. Soc.* 127 (2005) 13100–13101.
- [6] J. Zhang, F.H.B. Lima, M.H. Shao, K. Sasaki, J.X. Wang, J. Hanson, R.R. Adzic, *J. Phys. Chem. B* 109 (2005) 22701–22704.
- [7] D. Villers, X. Jacques-Bédard, J.-P. Dodelet, *J. Electrochem. Soc.* 151 (2004) A1507–A1515.
- [8] R. Bashyam, P. Zelenay, *Nature* 443 (2006) 63–66.
- [9] X. Bo, L. Guo, *Phys. Chem. Chem. Phys.* 15 (2013) 2459–2465.
- [10] Z. Yang, H. Nie, X.a. Chen, X. Chen, S. Huang, *J. Power Sources* 236 (2013) 238–249.
- [11] G. Liu, X. Li, P. Ganesan, B.N. Popov, *Appl. Catal., B: Environ.* 93 (2009) 156–165.
- [12] G. Liu, X. Li, P. Ganesan, B.N. Popov, *Electrochim. Acta* 55 (2010) 2853–2858.
- [13] C.W.B. Bezerra, L. Zhang, K. Lee, H. Liu, A.L.B. Marques, E.P. Marques, H. Wang, J. Zhang, *Electrochim. Acta* 53 (2008) 4937–4951.
- [14] C.H. Choi, S.H. Park, S.I. Woo, *J. Mater. Chem.* 22 (2012) 12107–12115.
- [15] E.N. Nxumalo, P.J. Letsoalo, L.M. Cele, N.J. Coville, *J. Organomet. Chem.* 695 (2010) 2596–2602.
- [16] H. Kim, K. Lee, S.I. Woo, Y. Jung, *Phys. Chem. Chem. Phys.* 13 (2011) 17505–17510.
- [17] H. Li, H. Liu, Z. Jong, W. Qu, D. Geng, X. Sun, H. Wang, *Int. J. Hydrogen Energy* 36 (2011) 2258–2265.
- [18] C.H. Choi, S.H. Park, S.I. Woo, *Appl. Catal., B: Environ.* 119–120 (2012) 123–131.
- [19] K. Sawai, N. Suzuki, *J. Electrochem. Soc.* 151 (2004) A682–A688.
- [20] X. Fu, Y. Liu, X. Cao, J. Jin, Q. Liu, J. Zhang, *Appl. Catal., B: Environ.* 130–131 (2013) 143–151.
- [21] R. Kothandaraman, V. Nallathambi, K. Artyushkova, S.C. Barton, *Appl. Catal., B: Environ.* 92 (2009) 209–216.
- [22] H.-S. Oh, J.-G. Oh, B. Roh, I. Hwang, H. Kim, *Electrochem. Commun.* 13 (2011) 879–881.
- [23] P.H. Matter, L. Zhang, U.S. Ozkan, *J. Catal.* 239 (2006) 83–96.
- [24] J.P. Paraknowitsch, J. Zhang, D. Su, A. Thomas, M. Antonietti, *Adv. Mater.* 22 (2010) 87–92.
- [25] J. Yuan, C. Giordano, M. Antonietti, *Chem. Mater.* 22 (2010) 5003–5012.
- [26] X. Tuayev, J.P. Paraknowitsch, R. Illgen, A. Thomas, P. Strasser, *Phys. Chem. Chem. Phys.* 14 (2012) 6444–6447.
- [27] J.P. Paraknowitsch, A. Thomas, M. Antonietti, *J. Mater. Chem.* 20 (2010) 6746–6758.
- [28] J.P. Paraknowitsch, A. Thomas, *Macromol. Chem. Phys.* 213 (2012) 1132–1145.
- [29] W. Yang, T.-P. Fellingner, M. Antonietti, *J. Am. Chem. Soc.* 133 (2011) 206–209.
- [30] H.-S. Oh, J.-G. Oh, W.H. Lee, H.-J. Kim, H. Kim, *Int. J. Hydrogen Energy* 36 (2011) 8181–8186.
- [31] C.H. Choi, S.Y. Lee, S.H. Park, S.I. Woo, *Appl. Catal., B: Environ.* 103 (2011) 362–368.

- [32] H.-S. Oh, H. Kim, *J. Power Sources* 212 (2012) 220–225.
- [33] G. Wu, C. Dai, D. Wang, D. Li, N. Li, *J. Mater. Chem.* 20 (2010) 3059–3068.
- [34] Y. Xia, R. Mokaya, *Chem. Mater.* 17 (2005) 1553–1560.
- [35] S. Yang, X. Feng, X. Wang, K. Mullen, *Angew. Chem. Int. Ed.* 50 (2011) 5339–5343.
- [36] H. Niwa, M. Kobayashi, K. Horiba, Y. Harada, M. Oshima, K. Terakura, T. Ikeda, Y. Koshigoe, J.-i. Ozaki, S. Miyata, S. Ueda, Y. Yamashita, H. Yoshikawa, K. Kobayashi, *J. Power Sources* 196 (2011) 1006–1011.
- [37] X. Bao, X. Nie, D. Deak, E. Biddinger, W. Luo, A. Asthagiri, U. Ozkan, C. Hadad, *Top. Catal.* 56 (2013) 1623–1633.